FLOW AND HEAT TRANSFER IN OUTLET PIPES OF CRYOSTATTING SYSTEMS

V. A. Babenko

UDC 621.3.045:536.483

Flow and heat transfer at mixed convection in the vertical channel connecting a cryogenic vessel and a room temperature zone are considered. The two-dimensional problem of conjugated heat transfer in the metal wall of the channel and in its cavity is solved by the finite difference method. The calculated values of the heat flux into the cold zone and of the temperature of the hot pipe end at different channel wall thicknesses, lengths, diameters, helium flowrates, as well as at different constants of the interaction of heat with the environment are given.

The outlet pipe of the cryostatting system for the helium temperature level can initiate considerable heat fluxes into the cold cryostat zone under certain conditions. This problem is also significant for a gas-cooled cryogenic current lead, whose element can be considered as a pipe, with its wall being electrically heated. Strictly speaking, this study is concerned with a pipe since the shape of gas channels in real designs of cooled current leads may be sufficiently complex.

In the available publications dealing with current lead calculations, metal-to-coolant heat transfer coefficients are assigned a priori, laying stress on optimization of geometrical sizes under sufficiently good or ideal heat transfer. Theoretically, the problem of providing such heat transfer conditions is not considered.

In the majority of cases, the experimentally measured heat fluxes into the cold zone for current leads greatly exceed the design ones [1]. Such a difference can be caused by the fact that the contribution of free convection imposed on forced flow has not been taken into account. Meanwhile, this mechanism is insufficiently studied in publications on cooling of heat bridges and current leads.

Usually, flow from cryogenic vessels occurs at low Reynolds numbers, and temperature drops both in the longitudinal direction (hot end — cold end) and in the cross direction (flow axis — heated wall) attain a hundred degrees. These circumstances and the specific features of helium thermophysical properties result in conditions for mixed convection to occur in outlet pipes.

The previous publication [2] is concerned with calculation results for a nonelectrically heated pipe. The present work considers a wall-heated pipe.

The mathematical statement of the problem includes the Navier–Stokes continuity equation and the heat transfer equation in a cylindrical coordinate system

$$\frac{\partial}{\partial x}(r\rho u) + \frac{\partial}{\partial r}(r\rho v) = 0, \tag{1}$$

$$\frac{\partial}{\partial x}(r\rho u^2) + \frac{\partial}{\partial r}(r\rho vu) = -r\frac{\partial P}{\partial x} + \frac{\partial}{\partial x}\left(r\mu\frac{\partial u}{\partial x}\right) + \frac{\partial}{\partial r}\left(r\mu\frac{\partial u}{\partial r}\right) + r\frac{\partial}{\partial x}\left(\mu\frac{\partial u}{\partial x}\right) + \frac{\partial}{\partial r}\left(r\mu\frac{\partial v}{\partial x}\right) - \rho g, \tag{2}$$

$$\frac{\partial}{\partial x}(r\rho uv) + \frac{\partial}{\partial r}(r\rho v^2) = -r\frac{\partial P}{\partial r} + \frac{\partial}{\partial x}\left(r\mu\frac{\partial v}{\partial x}\right) + \frac{\partial}{\partial r}\left(r\mu\frac{\partial v}{\partial r}\right) + r\frac{\partial}{\partial x}\left(\mu\frac{\partial u}{\partial r}\right) + \frac{\partial}{\partial r}\left(r\mu\frac{\partial v}{\partial r}\right) + \frac{2\mu v}{r}, \tag{3}$$

A. V. Lykov Heat and Mass Transfer Institute, Academy of Sciences of Belarus, Minsk. Translated from Inzhenerno-fizicheskii Zhurnal, Vol. 63, No. 6, pp. 665-672, December, 1992. Original article submitted June 6, 1991.

 1062-1025/92/6306-1176$12.50

$$\frac{\partial}{\partial x}(r\rho u c_p T) + \frac{\partial}{\partial r}(r\rho v c_p T) = \frac{\partial}{\partial r}\left(r\lambda \frac{\partial T}{\partial r}\right) + \\ + \frac{\partial}{\partial x}\left(r\lambda \frac{\partial T}{\partial x}\right) + \mu r\left(\frac{\partial u}{\partial r}\right)^2 + ru\frac{\partial P}{\partial x} \tag{4}$$

subject to the boundary conditions: on the cold pipe end at x = 0

$$u = u_0,\ v = 0,\ T = T_0, \tag{5}$$

on the hot pipe end at x = L and within a < r < b

$$-\lambda \frac{dT}{dx} = \alpha_1 (T_1 - T_e), \tag{6}$$

on the hot pipe end at x = L and within 0 < r < a

$$\frac{\partial u}{\partial x} = 0,\quad \frac{\partial T}{\partial x} = 0,\ v = 0, \tag{7}$$

on the inner pipe surface r = a

$$\lambda \frac{\partial T}{\partial r}\bigg|_{r=r^-} = \lambda \frac{\partial T}{\partial r}\bigg|_{r=r^+},\ u = 0,\ v = 0, \tag{8}$$

on the outer pipe surface r = b

$$-\lambda \frac{dT}{dr} = \alpha_3 (T_3 - T_0), \tag{9}$$

on the symmetry axis r = 0

$$\frac{\partial u}{\partial r} = 0,\quad \frac{\partial T}{\partial r} = 0,\ v = 0. \tag{10}$$

Boundary conditions (6) and (9) are generalizations of the more frequently reported conditions for ideal heat transfer on the hot end $T_1 = T_e$ and of the conditions for no-background heat input in the cryostat $q_3 = 0$.

The problem of the type of boundary condition at $x = x_1$ is ambiguous. In a correctly designed current lead the condition $T_1 = T_e$ is satisfied, however, rather not due to a great coefficient for the interaction between heat and surrounding medium α_1, but due to a successfully chosen relation between the longitudinal size of the current lead and the cross section of a current-conducting metal wall. On the other hand, in practice the condition $T_1 = T_e$ is more frequently violated since, first, the service conditions (i.e., current and flowrate) can differ from the design ones and, second, the empirical knowledge about the heat transfer coefficient included into the design of the current lead in terms of this or that optimization may not conform to reality.

The system of equations (1)-(4) with the boundary conditions was solved by Patankar's method [3] as described in [2]. Sebesi and Smith's model [4], being most complete among the algebraic ones and well checked for tube flow, was used to calculate effective values of the viscosity coefficient and thermal conductivity.

Helium thermophysical properties were assigned allowing for tabular data [5], and we considered copper M1 as the pipe wall material, whose approximate physical properties were given in [1].

The present study is mainly aimed at revealing the specific features of flow and heat transfer that follow from the two-dimensional nature of processes and are bound up with vortex formation, which cannot be taken into account in the one-

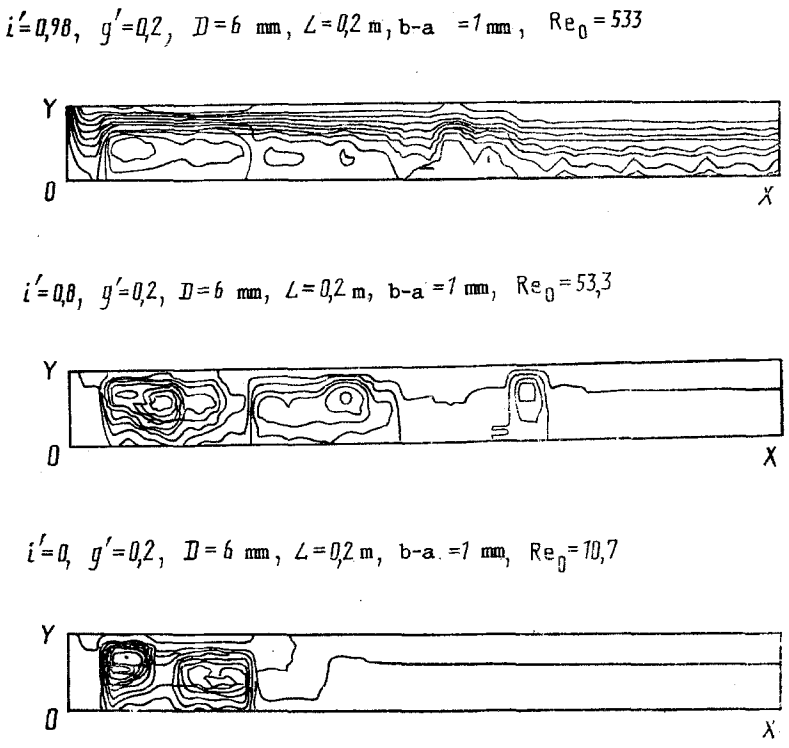

Fig. 1. Streamlines: on the left, cold end; on the right, hot end; at the bottom, symmetry axis; from above, wall.

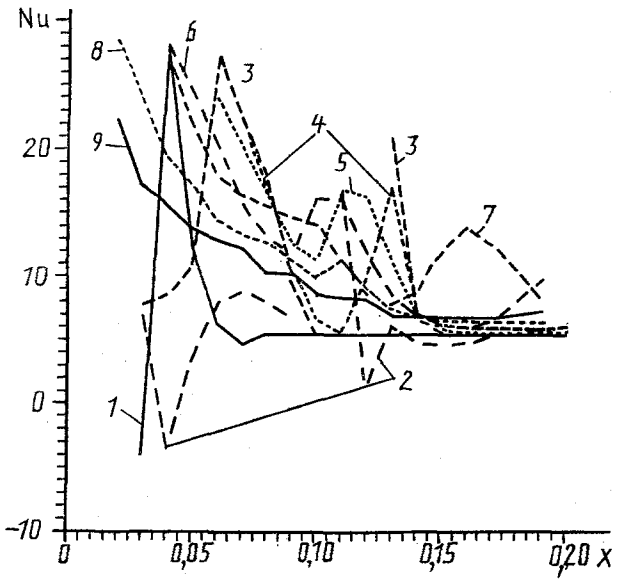

Fig. 2. Nusselt number $Nu = \alpha_2 D/\nu$ vs current and longitudinal coordinate at $g' = 0.2$, $D = 6$ mm, $L = 0.2$ m, $b - a = 1$ mm, $\alpha_1 = 100$ W/(m^2 ·K): 1) $i' = 0$; 2) 0.4; 3) 0.8; 4) 0.9; 5) 0.95; 6) 0.96; 7) 0.97; 8) 0.98; 9) $i' = 0.988$.

dimensional models. Along with the above-mentioned two-dimensional model, comparison with the one-dimensional calculation and generalization of the results will require the one-dimensional heat transfer model to be written down, too.

As usual, the one-dimensional heat transfer model is obtained by averaging over the channel cross section and its wall and by including heat transfer coefficients in Eq. (4):

$$Gc_p \frac{dT_q}{dx} = \alpha_2 \Pi_2 (T_w - T_g) + \alpha_3 \Pi_3 (T_w - T_9), \tag{11}$$

$$\frac{dQ}{dx} = -\frac{\varkappa I^2}{S} + \alpha_2 \Pi_2 (T_w - T_q), \tag{12}$$

$$\Lambda S \frac{dT_w}{dx} = Q. \tag{13}$$

The boundary conditions are:

$$\text{at} \quad x = 0: \; T_g = T_w = T_0, \quad \text{at} \quad x = L: \; Q = \alpha_1 S (T_e - T_1). \tag{14}$$

To reduce the model to a dimensionless form the following system of dimensionless criteria and coordinates:

$$g' = \frac{Gc_{pe}}{N}, \; i' = \frac{L_e^{1/2} I}{N}, \; s' = \frac{S\Lambda_e}{LN}, \; x' = \frac{xN}{S\Lambda_e}, \; t' = \frac{T_w - T_0}{\Delta T},$$

$$t_g' = \frac{T_g - T_0}{\Delta T}, \; \vartheta' = \frac{T_w - T_g}{\Delta T}, \; q' = \frac{Q}{\Delta TN}, \; \varkappa' = \frac{\varkappa \Lambda_e}{L_e \Delta T}, \; c_p' = \frac{c_p}{c_{pe}},$$

$$\Lambda' = \frac{\Lambda}{\Lambda_e}, \; \gamma_2 = \frac{\alpha_2 \Pi_2 \Lambda_e S}{N^2}, \; \gamma_3 = \frac{\alpha_3 \Pi_3 \Lambda_e S}{N^2}$$

has been taken. Here the subscript "e" refers to the environmental temperature T_e; $\Delta T = T_e - T_0$ is the temperature scale, and $N = L_e^{1/2} I + \alpha_1 S$ is the relative heat load scale.

The quantity N is the heat that enters the pipe or is released in it per unit temperature drop along the pipe. Use of this quantity as one of the main scales yields a unique generalization of the results both with and without electric current and allows the coefficient α_1 to be excluded in dimensionless form from the consideration.

Rewrite boundary-value problem (11)-(14) in dimensionless form

$$dq'/dx' = -i'^2 \varkappa' + \gamma_2 \vartheta' + \gamma_3 t', \tag{15}$$

$$dv'/dx' = q'/\Lambda' - \gamma_2 \vartheta'/g' c_p', \tag{16}$$

$$dt'/dx' = q'/\Delta', \tag{17}$$

$$x' = 0: \; t' = 0, \; \vartheta' = 0; \quad x' = x_1': \; q' = (1 - i')(1 - t'). \tag{18}$$

For a fixed temperature drop ΔT and the properties of the wall material and coolant $k'(T_w)$, $\Lambda'(T_g)$, and $c_p'(T)$ the dimensionless values of the current i', flowrate g', length x', and heat transfer coefficients γ_2 and γ_3 serve as the parameters of boundary value problem (15)-(18). The functions of these parameters are represented by the characteristic values of the dependent dimensionless variables q_0', t_1', and ϑ_1', as well as by the dimensionless index of energy consumptions spent for refrigeration $W' = W/(iL^{1/2}\Delta T)$, which is formulated from the similar dimensional quantity W calculated by the ideal thermodynamic Carnot cycle [1]

$$W = Gc_{pe} \left(T_e \ln \frac{T_{g1}}{T_0} - T_{g1} + T_0 \right) + \frac{\Delta T}{T_0} Q_0. \tag{19}$$

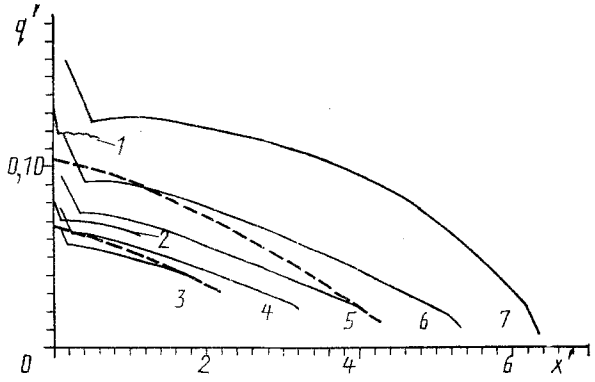

Fig. 3. Heat flux variation along the pipe at g′ = 0.2, D = 6 mm, b-a = 1 mm; α_1 = 100 W/(m^2 ·K): 1) I = 100 A; 2) 200; 3) 400; 4) 600; 5) 800; 6) 1000; 7) I = 1200 A.

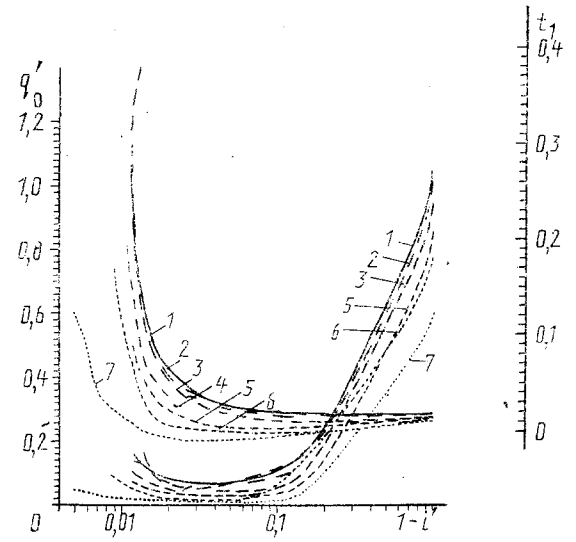

Fig. 4. Heat flux into the cold zone and the temperature of the hot pipe end at different currents and flowrates for the conditions of Fig. 3: 1) g′ = 0.2; 2) 0.5; 3) 1; 4) 3; 5) 5; 6) 10; 7) g′ = 20.

Let us present the calculation results.

1. Two-Dimensional Fields. Figure 1 shows the pattern of streamlines in the flow considered for three values of the dimensionless current parameter i′ at fixed geometrical sizes and fixed dimensionless flowrate g′. Different dimensional flowrates and Reynolds numbers correspond to these three values of g′. With increasing Reynolds number the vortex formation is suppressed; however, a coarse vortex in the vicinity of the cold pipe end takes place up to Re = 10^4 as in the case of the pipe with no wall heating earlier considered [2].

According to this pattern of streamlines, the flow isotherms are located so that in them there appear opposite slope sections where local heat transfer occurs from the more heated gas to the less heated wall. The characteristic form of the isotherms as well as of the isobars and lines of the equal density is shown in [2].

2. Nusselt Number vs the Coordinate along the Pipe. A sufficiently complex distribution pattern of the Nusselt number for heat transfer between the gas and wall along the pipe (Fig. 2) is the result of vortices present in the flow. If, for large values of i′ (great Re numbers correspond to them), a monotonic decrease of the Nusselt number along the entrance heat transfer section is observed, then for small i′ the Nusselt number distribution is nonmonotonic, and there are negative values and discontinuities bound up with the local equality of the temperatures T_g and T_w.

For illustration, the method of linear interpolation between points is used in Fig. 2. It should be borne in mind, however, that only the vortices of the broken curves possess the physical meaning. On the hot tube end the curves, to a con-

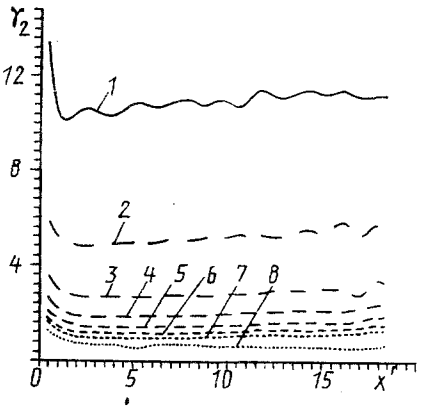

Fig. 5. Results on the parameter γ_2 calculated by the two-dimensional model at different pipe diameters: 1) D = 0.4 mm; 2) 1; 3) 2; 4) 3; 5) 4; 6) 5; 7) 6; 8) D = 9 mm ($g' = 5$, L = 0.4 m, $i' = 0.8$, $\alpha_1 = 1000$).

siderable extent, tend to the value of the Nusselt number characteristic of the completely developed velocity and temperature profiles in the laminar flow; on the cold pipe end a substantial scatter is observed. In decreasing i′ the value of the Nusselt number as a whole increases because the influence of the entrance heat transfer surface more strongly manifests itself at lower heating.

The heat flux distribution along the pipe is shown in Fig. 3. As the current grows the values of q_l' approach zero, charactersistic of the optimal current lead. In practice, use of current leads with $q_l' = 0$ is, however, rather problematic since such conditions are indeed boundary-value in the sense of the existence of a steady-state solution. At a current greater than 1200 A (curve 7) and the mentioned geometrical sizes of the pipe wall the steady-state solution has not been obtained, and slow time growth of the temperature has been observed.

In Fig. 3 all the curves are characterized by sharp growth of the heat flux while approaching the cold pipe end. As mentioned above, this growth is the cause of the wall zones with an opposite flow direction present in the gas flow and results in a 20-30% increase of the heat flux into the cold zone. For comparison, in Fig. 3 the dashed lines denote the calculation results obtained by the one-dimensional model (16)-(18) for two values of the current corresponding to curves 3 and 5. In one-dimensional model calculations, the heat transfer coefficient is taken constant and corresponding to the one calculated by the one-dimensional model at x = L. In the case of the one-dimensional calculation the heat flux lines lie higher close to the cold end because the cooling intensity is higher at the pipe entrance in virtue of the entrance section influence on heat transfer.

The current-carrying wall-mean temperature distribution for the conditions in Fig. 3 yields at small i′ an exponential temperature growth along the longitudinal coordinate characteristic of the short current lead, as compared to the optimal one. As the current increases the current lead becomes closer to the optimal one, i.e., to the corresponding condition of $q_l' = 0$. For the wall temperature distributions corresponding to curves 6 and 7 in Fig. 3, the curves t′(x′) are markedly smoothed near the hot pipe end.

3. Dependences on the Pipe Length. The calculation results by the one-dimensional model (15)-(18), where the parameters γ_2, γ_3, and i′ are fixed and the parameters g′ and x_l' are varied, have shown that while approaching some pipe length, limiting for a given flowrate, the temperature of the hot pipe end quickly grows. For a pipe exceeding this length the steady-state solution has not been obtained because it is bound up with unsteady heating under these cooling conditions. It is found that for insufficiently intensive cooling the condition $t_l' = 1$ cannot be attained at any length and flowrate.

Usually current leads are optimized by one of two criteria [1]: $q_0' \to \min$ or $W' \to \min$. Let us describe qualitatively the dependences $q_0'(x_l')$ and $W'(x_l')$.

At $x_l' \to 0$ the current lead is indeed noncooled. As a result, the curves tend to the same value, equal to $q_l' = 1 - i'$. The curves $q_0'(x_l')$ have a minimum, whose depth and relative sharpness depend on the flowrate. Directly behind this minimum, when x_l' increases, the region of sharp growth of the heat flux is located and it is bound up with the boundary of

the existence of the steady-state solution. At great flowrates the minimum is not sharp, and a steady-state solution exists over a greater range of x_1'.

The behavior of the dependences $W'(x_1', g')$ qualitatively repeats the course of the dependences $q_0'(x_1', g')$ except in the case where the minimum of energy consumptions does not degenerate at great g'.

4. Flowrate Characteristics. When g' tends to zero ($g' < 0.1$) the scatter in the dependence $q_0'(g', \gamma_2)$ with respect to the parameter γ_2 is absent, which conforms to a transition to the limit of a noncooled current lead. For an asymptotically great flowrate ($g' > 5$) the values of q_0' are practically constant and depend on γ_2 alone. Low values of heat fluxes ($q_0' < 0.01$) can be attained at $\gamma_2 > 8$.

Energy consumption dependences on the flowrate show that in the plots of $W'(g')$ there exist two minima, the first minimum at $q' \approx$ 1-1.5 being more clearly pronounced for great values of i'. Earlier in [2, 6] the energy consumption dependences on the flowrate with one minimum are described. The difference in the statement of the problem is apparently the reason of such a disagreement. For the boundary condition on the hot end (18) the temperature is not fixed rigidly. Copper thermal conductivity as a function of temperature over a low-temperature range is nonmonotonic, and this results in the existence of two minima.

5. Current Characteristics. The heat flux q_1 on the hot pipe end depends mainly on the current i' and weakly depends on the flowrate g', i.e., calculation, in fact, yields the universal curve $q_1'(g')$. Note that this does not follow from the form of boundary condition (18). As is seen from Fig. 4, the temperature of the hot pipe-wall end and the heat flux into the cold zone depend, to a considerable extent, on the flowrate. In decreasing the current i' from unity there occurs a decrease in the temperature t_1'; however, in the small i' region the temperature t_1' increases again.

Figure 4 presents results calculated by the one-dimensional model when geometrical sizes and the heat transfer coefficient on the hot end are fixed. The heat transfer intensity parameter γ_2 is variable both along the pipe and when varying the current from version to version.

6. Dependences on the Pipe Diameter. Let us analyze the dimensionless heat transfer intensity parameter γ_2 vs the channel diameter D. Figure 5 plots the parameter γ_2 distribution along the pipe. Behind the small-length entrance section there occurs a slow increase of γ_2, on which irregular oscillations are imposed. As follows from the results calculated by the one-dimensional model the low values of energy consumptions and heat fluxes into the cold zone can be attained only at $\gamma_2 > 8$-10. For this, the channel diameter must be at least smaller than 0.4 mm (Fig. 5). When the diameter decreases up to such values, the heat flux into the cold zone reduces to $q_0' = 0.01$, which is consistent with the dimensional values of the reduced heat fluxes $Q/I \leq 0.4$ mW/A. Although these estimates can vary by changing the current and flowrate parameters, they nevertheless can be the basis for choosing the current lead design parameters.

NOTATION

L, pipe length; Q, wall heat flux; T_w, mean wall temperature; T_g, mean gas temperature; G, gas flowrate; Π, heat transfer perimeter; $\varkappa$, specific resistance; I, current; S, wall cross section; Λ, wall thermal conductivity; $L_e = 2.45 \times 10^{-8}$, Widemann-Franz number.

REFERENCES

1. I. A. Glebov, V. N. Shakhtarin, and Yu. F. Antonov, Problem of Current Input into Superconducting Devices [in Russian], Leningrad (1985).
2. V. A. Babenko, Low-Temperature Heat and Mass Transfer Processes in Energy Saving Technologies [in Russian], Minsk (1990), pp. 17-30.
3. S. Patankar, Numerical Heat Transfer and Fluid Flow, Hemisphere, New York (1980).
4. T. Sebesi and P. Bredshou, Convective Heat Transfer [Russian translation], Moscow (1987).
5. R. D. McCarty, NBS Technical Notes, No. 631 (1972).
6. L. L. Vasil'ev, G. I. Bobrova, V. A. Babenko, et al., Cryogenic Current Leads, Preprint of Heat and Mass Transfer Institute, No. 18, Minsk (1983).